 CMES, vol.5, no.2, pp.135-149, 2004

Homogenization Analysis for Particulate Composite Materials using the Boundary Element Method

Hiroshi Okada[1], **Yasuyoshi Fukui**[1] **and Noriyoshi Kumazawa**[1]

Abstract: A method to obtain the effective mechanical properties of particulate composite materials is presented in this paper. The methodology is based on the boundary element method (BEM) coupled with analytical solutions for ellipsoidal inclusions such as Eshelby's tensor. There is no numerical integration for the surfaces or the domains of distributed particles, and, therefore, proposed technique is very efficient. Homogenization analysis based on representative volume element (RVE) is carried out considering a unit cell containing many particles (up to 1000). By using a conventional BEM approach (i.e., multi-region BEM), it would be extremely difficult to analyze such a large RVE, since the problem size would become unacceptably large. Some numerical solutions are presented and the accuracy of present approach is discussed in this paper.

keyword: Boundary element method (BEM), Homogenization method, Representative volume element (RVE), Ellipsoidal inclusion, Eshelby's tensor.

1 Introduction

So far, a number of applications of homogenization analyses have been presented. Homogenization method can be used as an analytical engine to connect the results of unit cell analysis for the microstructure of heterogeneous materials and the macroscopic mechanical properties. For example, macroscopic elastic moduli of heterogeneous materials can be evaluated by the homogenization method (Guedes & Kikuchi (1990); Kalamkarov (1992); Hollister & Kikuchi (1994)). Effective mechanical behaviors of composites materials whose material constituents undergo material and geometric nonlinear behavior can be determined by the homogenization analyses (Okada, Fukui, Kumazawa & Maruyama (1998); Wu & Ohno (1999); Ohno, Wu & Matsuda (2000); Ohno, Matsuda & Wu (2001); Ohono, Okumura & Noguchi (2002); Takano, Ohnishi, Zako & Nishiyabu (2000); Takano, Ohnishi, Zako & Nishiyabu (2001); Higa & Tomita (2000)) and also the effective mechanical properties of structural components can be evaluated (Okada, Fujitani, Fukui & Kumazawa (2001); Takano, Zako & Kikuchi (1995)). Analysis/design for smart material/structure can be done by the homogenization method (Silva, Nishiwaki, Fonseca & Kikuchi (1999)). The homogenization method is quite versatile and has applied to many types of problems and is considered to be a very important member among the methods of multi-scale analysis such as S-version FEM (Fish (1992); Fish & Guttal (1996)). As a latest development in the context, Raghavan & Ghosh (2004) presented an adaptive strategy that can vary computational resolution for critical and non-critical regions.

So far, the most of homogenization analyses have been carried out using the finite element method (FEM). As a numerical method, the boundary element method (BEM) should be able to be used for the homogenization analyses. However, only a few homogenization analyses have been presented in literature (Shibuya & Wang (1994); Kaminski (1999); Procházka (2001); Okada, Fukui & Kumazawa (2000, 2001a, 2002)). Therefore, the advantages and disadvantages of BEM in the analyses of homogenization method have not fully been explored. The authors' previous papers have presented some results of homogenization analyses using BEM. Two different formulations have been presented for the homogenization analyses based on BEM (single-region BEM with volume integral terms to represent the difference between the matrix material and other material constituents and multi-region BEM (Okada, Fukui & Kumazawa (2001a, 2002))).

On the other hand, particulate composite materials as depicted in **Figure 1** contain second phase particles which are distributed randomly or regularly in matrix material (see Ashby (1993) for a comprehensive review of

[1] Kagoshima University, Kagoshima, Japan

composite materials). The overall mechanical properties are improved compared with monotonic materials (i.e., higher value of elastic modulus, etc.). To evaluate the effective mechanical properties of particulate composites, representative volume element (RVE) approaches based on FEM have often been used. RVE approaches include the homogenization method. In many cases, only one or several particles are typically distributed in an RVE (for example, Wienecke, Brockenbrough & Romanko (1995); Higa & Tomita (2000)), or two dimensional idealization is adopted (Terada, Hori, Kyoya & Kikuchi (2000)). For the problems in which the particles distribute randomly in a three dimensional space, we need to assume the distribution of a number of particles in an RVE. Carrying out such analysis by assuming tens and hundreds of randomly distributed particles in an RVE would be troublesome not only in carrying out the computation itself but also in generating its input data. Though image based finite element method (Hollister & Kikuchi (1992), Terada, Miura & Kikuchi. (1997)) or Vronoi cell finite element method (Moorthy & Ghosh (1998) and Lee Moorthy & Ghosh (1999)) may be used to simplify the processes of model generation, the problems associated with the problem size still remain.

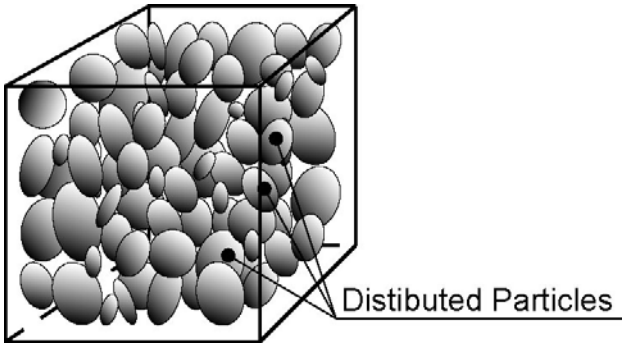

Figure 1 : Particulate composite material composed of matrix and embedded particles

In present research, we propose a homogenization analysis methodology by using the boundary element method (BEM) for particulate composite material (**Figure 1**). BEM was invented in the late 60thby the pioneers (Rizzo (1967); Cruse (1969)) and has evolved over the years expanding its capabilities from linear to nonlinear analyses (Banerjee & Cathie (1980); Banerjee & Reveendra (1987), Chandra & Mukherjee (1983, 1986); Okada, Rajiyah & Atluri (1988, 1989); Okada & Atluri (1994)). Also, a fundamental development to obtain weakly singular traction and displacement boundary integral equations was recently presented by Han & Atluri (2003). Incorporating the outcomes of such a methodology with those of present work may lead to very useful results. In the authors' previous papers (Okada, Fukui & Kumazawa (2001a, 2002)), the formulations and some numerical results of the homogenization analyses using BEM were presented. We found that the accuracy of analysis was unexpectedly good for coarse discretizations for the outer boundary of RVE domain and for volume/interface of the particle. With this in our mind, we further simplify the numerical method by using analytical solutions for particles and drastically reduce the amount of numerical computations. To this end, we assume the shapes of the distributed particles to be ellipsoidal and utilize available analytical solutions for ellipsoidal inclusions such as Eshelby's solutions (Eshelby (1957); Mura (1982)).

On the other hand works in similar lines of thought can be found in literature. Nishioka and Kato (1998) and Kato and Nishioka (2000) has presented a numerical method using analytical solutions for embedded cracks and the problems of microcracked solid were analyzed. A number of microcracks were assumed to exist in the analysis domain. Banerjee & Henry (1992) presented a formulation of BEM for the analysis of fiber reinforced composites, in which the integrals of surface of fibers were reduced to one dimensional line integral. Essential idea that integrals are somehow simplified is quite similar to that in present work.

In this paper, we first present the formulations of homogenization analysis using BEM and then its extension to the analysis of particulate composite materials is discussed. We present some numerical solutions for the variations of effective elastic moduli of composite and internal stress distributions. It is shown that analyses for a unit cell containing 1000 particles can be carried out by present BEM approach.

2 Integral equations for homogenization method for particulate composite material

2.1 Preliminary

Some general remarks on the formulations of homogenization method are discussed by following Kalamkarov (1992). It is noted that there are many other key literature in the subject such as Bensoussan, Lions & Papanicolaou

(1978). Global structure is assumed to be composed of periodic microstructures as shown in **Figure 2**. The size ε of unit cell is considered to be very small compared with that of the global structure. The displacements u_i are expressed in terms of global coordinates x_i and local coordinates y_i. And they are related through the size ε of unit cell,:

$$y_i = x_i/\varepsilon + c_i \tag{1}$$

The displacements u_i are expressed by an asymptotic expansion.

$$u_i(\mathbf{x},\mathbf{y}) = u_i^o(\mathbf{x},\mathbf{y}) + \varepsilon u_i^1(\mathbf{x},\mathbf{y}) + \varepsilon^2 u_i^2(\mathbf{x},\mathbf{y}) + +\varepsilon^3 u_i^3(\mathbf{x},\mathbf{y})\cdots \tag{2}$$

Equation formulations governing the deformations of solid at local and global level are derived in a limiting sense that the size ε of unit cell is infinitesimally small (i.e., $\varepsilon \to 0$).

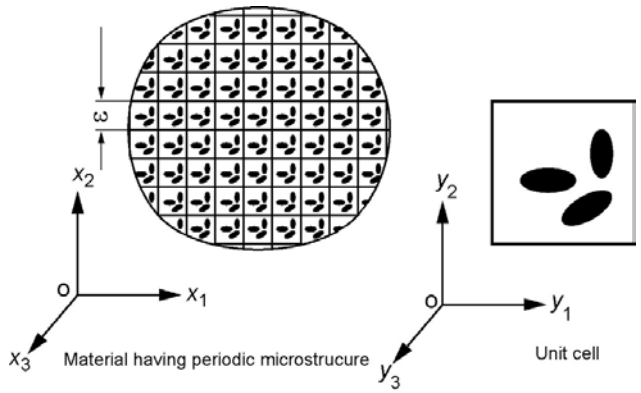

Figure 2 : A heterogeneous material having periodic microstructure

The structure is composed of matrix and embedded secondary phase materials as illustrated for a unit cell in **Figure 3**. As shown in **Figure 3**, the secondary phase materials are embedded in the unit cell and, therefore, the elastic constants $E_{ijk\ell}$ are expressed as functions of local coordinates y_i.

$$\begin{aligned} &E_{ijk\ell} = E^M_{ijk\ell}\ \left(y_i \in\ Y - \left[Y^{*1} + Y^{*2} + Y^{*3} + \cdots + Y^{*N}\right]\right) \\ &E_{ijk\ell} = E^{*1}_{ijk\ell}\ \left(y_i \in\ Y^{*1}\right),\ E_{ijk\ell} = E^{*2}_{ijk\ell}\ \left(y_i \in Y^{*2}\right), \\ &E_{ijk\ell} = E^{*3}_{ijk\ell}\ \left(y_i \in Y^{*3}\right),\ \cdots,\ E_{ijk\ell} = E^{*N}_{ijk\ell}\ \left(y_i \in Y^{*N}\right) \end{aligned} \tag{3}$$

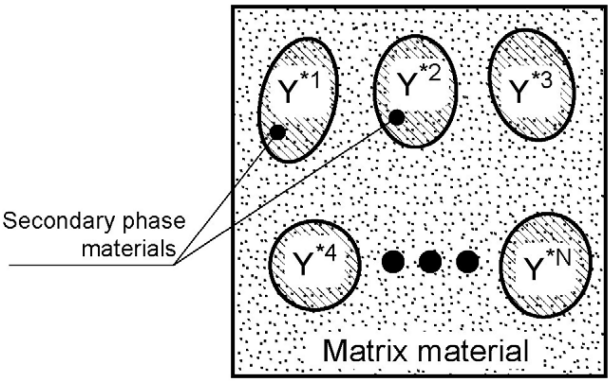

Figure 3 : Heterogeneous material composed of matrix and embedded second phase materials

where $Y^{*I}\,(I = 1,2,3,\cdots,N)$ represents the domain of the I-th secondary phase material. In this paper, we assume that matrix material is elastic and is homogeneous and isotropic. The secondary phase materials are elastic and homogeneous within a material phase but need not be isotropic.

The stresses are expressed by Hooke's law. The equation of equilibrium (linear momentum balance law) are to be satisfied in the solid. They are written to be:

$$\sigma_{ij} = E_{ijk\ell}\frac{\partial u_k}{\partial x_\ell} \tag{4}$$

$$\frac{\partial \sigma_{ij}}{\partial x_i} + b_j = 0 \tag{5}$$

where b_i are the body force per unit volume.

The derivatives of the displacements u_i are written to be:

$$\begin{aligned} \frac{\partial u_i}{\partial x_j} &= \frac{\partial u_i^o(\mathbf{x},\mathbf{y})}{\partial x_j} + \varepsilon\frac{\partial u_i^1(\mathbf{x},\mathbf{y})}{\partial x_j} + \varepsilon^2\frac{\partial u_i^2(\mathbf{x},\mathbf{y})}{\partial x_j} + \varepsilon^3\frac{\partial u_i^3(\mathbf{x},\mathbf{y})}{\partial x_j} \\ &\quad + \cdots + \frac{1}{\varepsilon}\frac{\partial u_i^o(\mathbf{x},\mathbf{y})}{\partial y_j} + \frac{\partial u_i^1(\mathbf{x},\mathbf{y})}{\partial y_j} + \varepsilon\frac{\partial u_i^2(\mathbf{x},\mathbf{y})}{\partial y_j} \\ &\quad + \varepsilon^2\frac{\partial u_i^3(\mathbf{x},\mathbf{y})}{\partial y_j} + \cdots \end{aligned} \tag{6}$$

We then use Eq. 6 in Eqs. 4 and 5 and we arrive at:

$$\frac{\partial}{\partial x_i}\left[E_{ijk\ell}\left(\frac{\partial u_k^o}{\partial x_\ell}+\frac{\partial u_k^1}{\partial y_\ell}\right)\right]+\frac{\partial}{\partial y_i}\left[E_{ijk\ell}\left(\frac{\partial u_k^1}{\partial x_\ell}+\frac{\partial u_k^2}{\partial y_\ell}\right)\right]$$
$$+\varepsilon(\cdots)+b_j$$
$$+\frac{1}{\varepsilon}\left\{\frac{\partial}{\partial x_i}\left[E_{ijk\ell}\frac{\partial u_k^o}{\partial y_\ell}\right]+\frac{\partial}{\partial y_i}\left[E_{ijk\ell}\left(\frac{\partial u_k^o}{\partial x_\ell}+\frac{\partial u_k^1}{\partial y_\ell}\right)\right]\right\}$$
$$+\frac{1}{\varepsilon^2}\frac{\partial}{\partial y_i}\left[E_{ijk\ell}\frac{\partial u_k^o}{\partial y_\ell}\right]=0 \tag{7}$$

In Eq. 7, the terms are organized according to the orders of ε. In order for Eq. 7 to be unconditionally bounded in the limit $\varepsilon\to 0$, the coefficients of $1/\varepsilon$ and $1/\varepsilon^2$ need to be zero. Therefore, we write:

$$\frac{\partial}{\partial x_i}\left[E_{ijk\ell}\frac{\partial u_k^o}{\partial y_\ell}\right]+\frac{\partial}{\partial y_i}\left[E_{ijk\ell}\left(\frac{\partial u_k^o}{\partial x_\ell}+\frac{\partial u_k^1}{\partial y_\ell}\right)\right]=0$$
$$\frac{\partial}{\partial y_i}\left[E_{ijk\ell}\frac{\partial u_k^o}{\partial y_\ell}\right]=0 \tag{8}$$

For the second of Eq. 8 to be satisfied, we pose u_i^o to be the functions of global coordinates x_i only and they represent the deformation of global structure in the limit $\varepsilon\to 0$. Thus, we write:

$$u_i^o=u_i^o(\mathbf{x}) \tag{9}$$

$$\frac{\partial}{\partial y_i}\left[E_{ijk\ell}\left(\frac{\partial u_k^o}{\partial x_\ell}+\frac{\partial u_k^1}{\partial y_\ell}\right)\right]=0 \tag{10}$$

Eq. 10 is the governing equation for the analysis of unit cell. Assuming u_i^1 to be periodic functions about the y_i coordinates and neglecting higher order terms, we can arrive at governing equation for global analysis, as (see Kalamkarov (1992) for further details):

$$\frac{\partial}{\partial x_i}\left[\frac{1}{|Y|}\int_Y E_{ijk\ell}\left(\frac{\partial u_k^o}{\partial x_\ell}+\frac{\partial u_k^1}{\partial y_\ell}\right)\mathrm{d}Y\right]+b_j=0 \tag{11}$$

Here, Y and $|Y|$ the region of unit cell and its volume in the y_i coordinate system.

For a specified macroscopic deformation mode $(\partial u_j^o/\partial x_k)$, a unit cell analysis can be carried out and the displacements u_i^1 can be obtained. u_i^1 are expressed in terms of $\partial u_j^o/\partial x_k$ and functions $F_{ijk}(\mathbf{y})$, as:

$$u_i^1=F_{ijk}(\mathbf{y})\frac{\partial u_j^o}{\partial x_k} \tag{12}$$

Thus, from Eq. 11, effective elastic moduli can be given to be:

$$E_{ijk\ell}^H=\frac{1}{|Y|}\int_Y\left[E_{ijk\ell}+\frac{1}{2}E_{ijmn}\left(\frac{\partial F_{mk\ell}}{\partial y_n}+\frac{\partial F_{m\ell k}}{\partial y_n}\right)\right]\mathrm{d}Y \tag{13}$$

2.2 Integral equations for unit cell analysis in homogenization method

Here a formulation of homogenization method based on the single-region BEM (Okada, Fukui & Kumazawa (2001a, 2002)) is briefly described. A method of weighted residuals is used and the weak form of the governing equation is written for the region of unit cell, as:

$$\int_Y\left\{\frac{\partial}{\partial y_i}\left[E_{ijk\ell}\left(\frac{\partial u_k^o}{\partial x_\ell}+\frac{\partial u_k^1}{\partial y_\ell}\right)\right]\right\}w_j\,\mathrm{d}Y=0 \tag{14}$$

where w_j are the weighting functions and are the functions of local coordinates y_i. We then apply Gauss divergence theorem and integrate Eq. 14 by parts, and we have:

$$0=\int_{\partial Y}t_jw_j\,\mathrm{d}(\partial Y)-\int_Y E_{ijk\ell}\frac{\partial}{\partial y_\ell}\left(y_m\frac{\partial u_k^o}{\partial x_m}+u_k^1\right)\frac{\partial w_j}{\partial y_i}\mathrm{d}Y \tag{15}$$

t_i are the tractions at the boundary of unit cell and are defined by:

$$t_j=n_iE_{ijk\ell}\left(\frac{\partial u_k^o}{\partial x_\ell}+\frac{\partial u_k^1}{\partial y_\ell}\right) \tag{16}$$

In deriving Eq. 15, we assume that traction equilibrium between different material constituents is satisfied. Eq. 15 is integrated by parts once more, and we obtain:

$$0=\int_{\partial Y}t_jw_j\,\mathrm{d}(\partial Y)-\int_Y E_{ijk\ell}^M\frac{\partial}{\partial y_\ell}\left(y_m\frac{\partial u_k^o}{\partial x_m}+u_k^1\right)\frac{\partial w_j}{\partial y_i}\mathrm{d}Y$$
$$-\sum_{I=1}^N\int_{Y^{*I}}\left(E_{ijk\ell}^{*I}-E_{ijk\ell}^M\right)\left(\frac{\partial u_k^o}{\partial x_\ell}+\frac{\partial u_k^1}{\partial y_\ell}\right)\frac{\partial w_j}{\partial y_i}\mathrm{d}Y^{*I} \tag{17}$$

Then we choose the weighting functions w_i to be Kelvin solution (Banerjee (1981), Kane (1994)) and an integral

equation for displacements u_i^1 is obtained.

$$
\begin{aligned}
&C_{pq}u_q^1(\xi_m) \\
&\quad = \int_{\partial Y} t_j u_{jp}^* \mathrm{d}(\partial Y) - \int_{\partial Y} u_k^1 t_{kp}^* \mathrm{d}(\partial Y) \\
&\qquad - C_{pq}\hat{u}_q^o(\xi_m) \; - \int_{\partial Y} \hat{u}_k^o t_{kp}^* \mathrm{d}(\partial Y) \\
&\qquad - \sum_{I=1}^{N} \int_{Y^{*I}} \left(E_{ijk\ell}^{*I} - E_{ijk\ell}^{M}\right) \frac{\partial \hat{u}_k}{\partial y_\ell} \frac{\partial u_{jp}^*}{\partial y_i} \mathrm{d}Y^{*I}
\end{aligned} \tag{18}
$$

Here, the components of displacement like vectors $\hat{u}_i^o$ and $\hat{u}_i$ are defined by:

$$
\hat{u}_i^o = y_j \frac{\partial u_i^o}{\partial x_j}, \quad \hat{u}_i = y_j \frac{\partial u_i^o}{\partial x_j} + u_i^1 \text{ and } \frac{\partial \hat{u}_i}{\partial y_j} = \frac{\partial u_i^o}{\partial x_j} + \frac{\partial u_i^1}{\partial y_j} \tag{19}
$$

Constants C_{pq} are determined depending on the location of the source point ξ_m. When the source point ξ_m is at the interior of domain Y, $C_{pq} = \delta_{pq}$ (δ_{pq} is the Kronecker's delta) and when ξ_m is at the smooth boundary of the domain $C_{pq} = \delta_{pq}/2$.

An expression for the displacement gradients is obtained by differentiating both the sides of Eq. 18 with respect to the coordinates of the source point ξ_m. When ξ_m is at the interior of region Y^{*J}, integral equation for the displacement gradients can be written to be:

$$
\begin{aligned}
&\frac{\partial \hat{u}_p(\xi_m)}{\partial \xi_q} \\
&\quad = \int_{\partial Y} t_j \frac{\partial u_{jp}^*}{\partial \xi_q} \mathrm{d}(\partial Y) - \int_{\partial Y} \frac{\partial t_{kp}^*}{\partial \xi_q} \hat{u}_k \mathrm{d}(\partial Y) \\
&\qquad - \sum_{I=1}^{N} \int_{Y^{*I}} \left(E_{ijk\ell}^{*I} - E_{ijk\ell}^{M}\right) \frac{\partial \hat{u}_k}{\partial y_\ell} \frac{\partial^2 u_{jp}^*}{\partial \xi_q \partial y_i} \mathrm{d}Y^{*I} \\
&\qquad - g_{pqij} \left(E_{ijk\ell}^{*J} - E_{ijk\ell}^{M}\right) \frac{\partial \hat{u}_k(\xi_m)}{\partial y_\ell} (\xi_m \in Y^{*J})
\end{aligned} \tag{20}
$$

Here the last term in the right hand side is called "free term" or "jump term" which arises due to the Cauchy principal value integral type singularity in the kernel function $\partial^2 u_{jp}^* / \partial \xi_q \partial y_i$ (see Banerjee & Butterfield (1981); Kane (1994); Okada Rajiyah & Atluri (1989)).

By discretizing the boundary of unit cell by the boundary elements and the interior of $Y^{*I}(I = 1, 2, 3, \cdots, N)$ by volume cells as shown in **Figure 4**, boundary element analysis for unit cell can be carried out (Okada, Fukui & Kumazawa (2001a, 2002)). In the analysis the displacements u_i^1 are to be determined for a specified macroscopic deformation mode $\partial u_i^o / \partial x_j$. Therefore, in Eq. 18, term associated with $\hat{u}_i^o \left(= y_j \partial u_i^o / \partial x_j\right)$ is regarded as the forcing term.

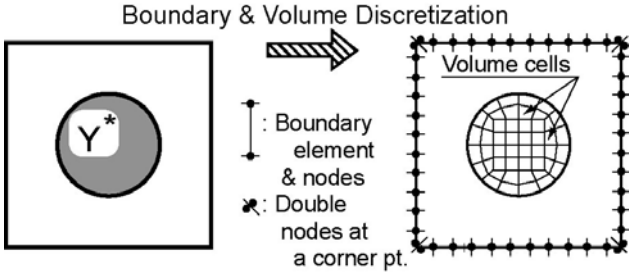

Figure 4 : Discretizations for the boundary of the unit cell and the interior of particles for single-region BEM formulation

2.3 Integral equations for the homogenization analysis of particulate composite material

In many micromechanics analyses, the particles and the distributions of strains within a particle are assumed to be ellipsoidal in their shapes and are uniform (see Mura (1982)). In present BEM formulation, we also adopt the assumptions of ellipsoidal inclusions (particles) and uniformly distributed strains. By adopting such assumptions, the volume integral terms in the integral Eqs. 18 and 20 can be simplified using available analytical expressions. The integrations are carried out based on the boundary elements and by the analytical solutions for ellipsoidal inclusions. By adopting the assumptions of uniform distributions of stresses and strains in each particle, the results of computation would be less accurate when the volume fraction of particles is large. In subsequent section, this issue is discussed with a simple numerical example.

We first define initial strain-like terms $\hat{\hat{\varepsilon}}_{ij}^I (I = 1, 2, 3, \cdots, N)$ in the particles, as:

$$
\begin{aligned}
\hat{\hat{\varepsilon}}_{ij}^I &= C_{ijmn}^M \left(E_{mnk\ell}^{*I} - E_{mnk\ell}^M\right) \frac{\partial \hat{u}_k^I}{\partial y_\ell} \\
&= C_{ijmn}^M \left(E_{mnk\ell}^{*I} - E_{mnk\ell}^M\right) \hat{\varepsilon}_{k\ell}^I
\end{aligned} \tag{21}
$$

where $\frac{\partial \hat{u}_k^I}{\partial y_\ell}$ and $\hat{\varepsilon}_{k\ell}^I$ are the displacement gradients and strains in the I-th particle, and they take constant values

within the particle. Thus, the volume integral terms are written to be:

$$\sum_{I=1}^{N}\int_{Y^{*I}}\left(E^{*I}_{ijk\ell}-E^{M}_{ijk\ell}\right)\frac{\partial\hat{u}_k}{\partial y_\ell}\frac{\partial u^*_j}{\partial y_i}\mathrm{d}Y^{*I} = \sum_{I=1}^{N}\hat{\hat{\varepsilon}}^I_{k\ell}\int_{Y^{*I}}E^{M}_{ijk\ell}\frac{\partial u^*_{jp}}{\partial y_i}\mathrm{d}Y^{*I} \tag{22}$$

It is found that the expression in the right hand side of Eq. 22 is nothing but the Green's function formula, which appears in the derivations for Eshelby's solution (see Eshelby (1957) and Mura (1982)). Following Mura (1982), analytical expressions for the integral $\int_{Y^{*I}}E^{M}_{ijk\ell}\frac{\partial u^*_j}{\partial y_i}\mathrm{d}Y^{*I}$ is obtained and we denote:

$$\Lambda^I_{pk\ell}=\int_{Y^{*I}}E^{M}_{ijk\ell}\frac{\partial u^*_{jp}}{\partial y_i}\mathrm{d}Y^{*I} \tag{23}$$

When the source point ξ_m is outside the domain Y^{*I} of the I-th particle, the expressions in $\Lambda^I_{k\ell}$ involve the Carlson's elliptic integrals of first and third kind and look somewhat troublesome. However, by use of mathematical subroutine libraries to evaluate the elliptic integrals (see Press, Teukolsky, Vetterling & Flannery (1996), for example), $\Lambda^I_{pk\ell}$ can be computed without any difficulties. The computation for $\Lambda^I_{pk\ell}$ is much faster than carrying out numerical integral for $\int_{Y^{*I}}E^{M}_{ijk\ell}\frac{\partial u^*_{jp}}{\partial y_i}\mathrm{d}Y^{*I}$. When the source point ξ_m is at the interior of Y^{*I}, $\Lambda^I_{pk\ell}$ are expressed by a linear functions of the coordinate values of ξ_m.

Thus, Eq. 18 can be rewritten to be:

$$C_{pq}u^1_q(\xi_m)=\int_{\partial Y}t_j u^*_{jp}\mathrm{d}(\partial Y)-\int_{\partial Y}u^1_k t^*_{kp}\mathrm{d}(\partial Y) -\int_{\partial Y}\hat{u}^o_k t^*_{kp}\mathrm{d}(\partial Y)\ -C_{pq}\hat{u}^o_q(\xi_m)-\sum_{I=1}^{N}\Lambda^I_{pk\ell}\hat{\hat{\varepsilon}}^I_{k\ell} \tag{24}$$

To evaluate the displacement gradients we differentiate both the sides of Eq. 24 with respect to the location ξ_m of the source point.

$$\frac{\partial\hat{u}_p(\xi_m)}{\partial\xi_q}=\int_{\partial Y}t_j\frac{\partial u^*_{jp}}{\partial\xi_q}\mathrm{d}(\partial Y)-\int_{\partial Y}\frac{\partial t^*_{kp}}{\partial\xi_q}\hat{u}_k\mathrm{d}(\partial Y) -\sum_{I=1}^{N}\frac{\partial\Lambda^I_{pk\ell}}{\partial\xi_q}\hat{\hat{\varepsilon}}^I_{k\ell} \tag{25}$$

Strains $\hat{\varepsilon}_{pq}$ which are the symmetric parts of $\partial\hat{u}_p/\partial\xi_q$ are expressed by:

$$\hat{\varepsilon}_{pq}(\xi_m)=\frac{1}{2}\int_{\partial Y}t_j\left(\frac{\partial u^*_{jp}}{\partial\xi_q}+\frac{\partial u^*_{jq}}{\partial\xi_p}\right)\mathrm{d}(\partial Y) -\frac{1}{2}\int_{\partial Y}\left(\frac{\partial t^*_{kp}}{\partial\xi_q}+\frac{\partial t^*_{kq}}{\partial\xi_p}\right)\hat{u}_k\mathrm{d}(\partial Y) -\sum_{I=1}^{N}\frac{1}{2}\left(\frac{\partial\Lambda^I_{pmn}}{\partial\xi_q}+\frac{\partial\Lambda^I_{qmn}}{\partial\xi_p}\right)\hat{\hat{\varepsilon}}^I_{mn} \tag{26}$$

When the source point ξ_m is at the interior of the J-th particle, Eshelby's tensor S^J_{pqmn} for the J-th particle appears from the last term in the right hand side of Eq. 26.

$$\hat{\varepsilon}_{pq}(\xi_m)=\frac{1}{2}\int_{\partial Y}t_j\left(\frac{\partial u^*_{jp}}{\partial\xi_q}+\frac{\partial u^*_{jq}}{\partial\xi_p}\right)\mathrm{d}(\partial Y) -\frac{1}{2}\int_{\partial Y}\left(\frac{\partial t^*_{kp}}{\partial\xi_q}+\frac{\partial t^*_{kq}}{\partial\xi_p}\right)\hat{u}_k\mathrm{d}(\partial Y) -\sum_{\substack{I=1\\I\neq J}}^{N}\frac{1}{2}\left(\frac{\partial\Lambda^I_{pmn}}{\partial\xi_q}+\frac{\partial\Lambda^I_{qmn}}{\partial\xi_p}\right)\hat{\hat{\varepsilon}}^I_{mn}-S^J_{pqmn}\hat{\hat{\varepsilon}}^I_{mn} \tag{27}$$

In Eqs. 25∼27, the volume integral terms in Eqs. 18 and 20 are replaced by analytical expressions.

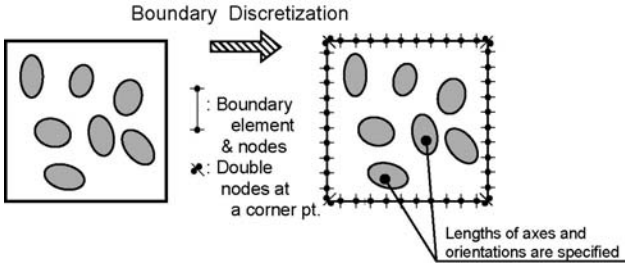

Figure 5 : Discretization for the boundary of the unit cell and the distributed particles

Discretizations for the boundary of unit cell and the distributed second phase particles are schematically illustrated in **Figure 5**. There is no volume cell to evaluate the domain integral. Only the shapes (lengths of three axes of ellipsoids) and the orientations of the axes are to be specified.

3 Numerical implementations for the unit cell analysis

In this section, the procedures of BEM analysis for the unit cell are discussed. However, the numerical evaluations of boundary integral terms are discussed briefly, since they are well known to the date (see, Banerjee & Butterfield (1981); Kane (1994), and other references are cited therein). We concentrate in some issues, which are particular of homogenization analysis. The periodic boundary conditions and iterative algorithm to obtain the solutions are discussed.

3.1 Boundary discretization for BEM unit cell analysis

The boundary of the unit cell is discretized by boundary elements. A three dimensional cubic or brick shaped unit cell is considered. The method of collocation is adopted to generate the system matrix by letting each boundary node be the source point one by one. Linear quadrilateral boundary element is adopted and 10 by 10 Gaussian quadrature is adopted. Although it is known that lower order Gaussian quadrature may be used for certain cases, we adopted the quadrature rule to assure the accuracy of integrals. Cauchy principal value type integrals are evaluated indirectly considering the rigid body translations and rotations. To represent discontinuities in tractions at corners of the unit cell, we adopt the method of double nodes, in which two or three nodes share the same location but have displacements and tractions independently (see **Figure 5** for the discretizations). Hence, one can generate a system matrix equation from Eq. 24, which looks like:

$$[G]\left\{u^1\right\} = [H]\{t\} - [G]\{\hat{u}^o\} + [Q]\{\hat{\varepsilon}\} \tag{28}$$

where $\left\{u^1\right\}$, $\{u^o\}$, $\{t\}$ are $\{\hat{\varepsilon}\}$ the column vectors consisting of the nodal values of u_i^1, u_i^o and t_i, and the strains $\hat{\varepsilon}_{ij}^I\,(I=1,2,3,\cdots,N)$ in the particles, respectively. In Eq. 28, we regard $\{u^o\}$ and $\{\hat{\varepsilon}\}$ to be the vectors of knowns, and $\left\{u^1\right\}$ and $\{t\}$ to be those of unknowns except for a few components in $\left\{u^1\right\}$. Matrices $[G]$, $[H]$ and $[Q]$ arise from the integrals in Eq. 24.

A matrix equation to evaluate the strains in the particles can be obtained from Eq. 27 and it can be shown, as:

$$\{\hat{\varepsilon}\} = \left[G'\right]\{\hat{u}\} + \left[H'\right]\{t\} + \left[Q'\right]\{\hat{\varepsilon}\} \tag{29}$$

where $\{\hat{u}\}$ represents the displacement-like quantities $\hat{u}_i$ at boundary nodes. Matrices $[G']$, $[H']$ and $[Q']$ arise from the integrals in Eq. 27.

3.2 Periodic boundary conditions and system matrix to be solved

In a homogenization analysis, the deformation of unit cell must be periodic. We enforce the periodic boundary conditions such that the displacements are continuous and traction reciprocity is satisfied between the neighboring unit cells. In a unit cell, the deformations have to be the same between the boundary planes which are facing each other, as shown in **Figure 6**. The traction reciprocity is enforced by letting the tractions on the paring planes be equal to each other but their signs are opposite. Thus, for a set of paring boundary nodes A and B in **Figure 7 (a)**, we can write:

$$\begin{aligned} &\left(u_i^1\right)^A = \left(u_i^1\right)^B, \quad \left[\left(u_i^1\right)^a = \left(u_i^1\right)^b\right] \\ &\text{and} \quad (t_i)^A + (t_i)^B = 0 \quad \left[(t_i)^a + (t_i)^b = 0\right] \end{aligned} \tag{30}$$

where $()^A \sim ()^J$ and $()^a \sim ()^q$ denote the quantities at the nodes A $\sim$ M and a $\sim$ q in **Figure 7**. In **Figure 7 (b)**, the faces of the cubical unit cell in **Figure 7 (a)** are opened for an illustrative purpose.

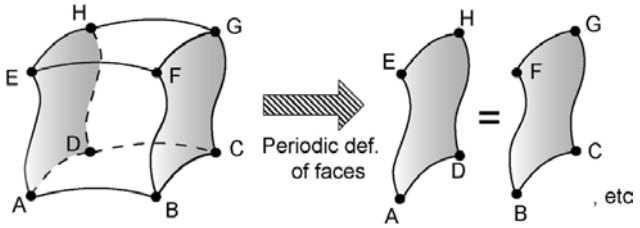

Figure 6 : Deformation of faces of unit cell under the assumption of periodic deformation

Unlike the case of FEM, in present BEM approach, we enforce the continuities of displacements and tractions in a continuing plane also. For example, displacements and tractions at nodes k and l in **Figure 7 (b)** have to be the same. Therefore, we also enforce conditions:

$$\left(u_i^1\right)^k = \left(u_i^1\right)^l \text{ and } (t_i)^k = (t_i)^l \tag{31}$$

However, nodes k and m in **Figure 7 (b)** share the same coordinates after the faces are assembled to be a cube,

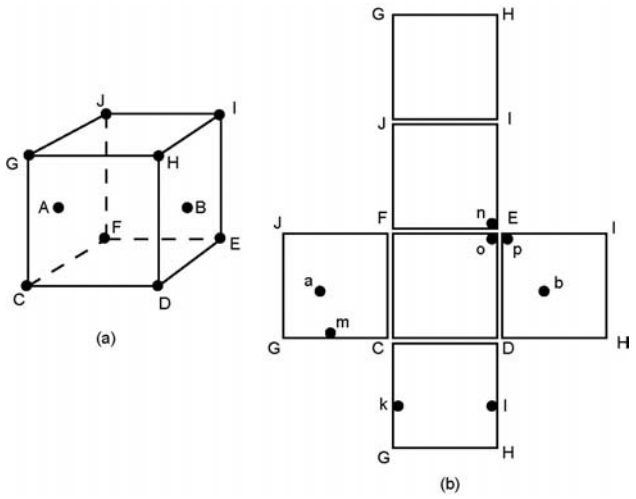

Figure 7 : A schematic illustration for how the periodic boundary conditions for the displacements and tractions are enforced

their nodal displacements and tractions are independent from each other due to the double node concept. Similarly, nodes *n*, *o* and *p* in **Figure 7 (b)** have the same location but their nodal quantities are independent from each other. We need to suppress the rigid body translation mode and constrain the displacements of a node at one of the eight convex points (nodes). Due to the conditions of Eqs. 30 and 31, all the nodes at the convex points must equal zero. Therefore, the displacements of nodes at points F∼M in **Figure 7** equal zero.

$$\begin{aligned}\left(u_i^1\right)^C &= \left(u_i^1\right)^D = \left(u_i^1\right)^E = \left(u_i^1\right)^F = \left(u_i^1\right)^G \\ &= \left(u_i^1\right)^H = \left(u_i^1\right)^I = \left(u_i^1\right)^J = 0\end{aligned} \tag{32}$$

By posing the conditions of Eqs. 30∼32 and appropriately rearrange the system matrices in Eq. 28, we can collect the unknown components of $\left\{u^1\right\}$ and $\{t\}$ in the left hand side. One can write:

$$[A]\{U\} = -[G]\{\hat{u}^o\} + [Q]\{\hat{\varepsilon}\} \tag{33}$$

where $\{U\}$ is consisting of unknown displacements and tractions at the boundary of unit cell. After the conditions Eqs. 30∼32 are enforced, the system matrix $[A]$ is no longer a square matrix. Number of simultaneous linear equations included in Eq. 33 is larger than the order of $\{U\}$. The reason is as follows. For example, there are 24 $(= 8 \times 3)$ equations generated by taking the eight convex points to be the source points. However, we have no degree of freedoms related to their displacements because all of them are constrained. By enforcing the condition of the second of Eq. 31, we only have 9 (3×3) independent traction components at those eight nodes. Therefore, the total number of unknown variables related to those nodes is 9 whereas we have 24 equations. Therefore, the system matrix $[A]$ in Eq. 33 is no longer a square matrix. To solve for unknown vector $\{U\}$ we use the least square method and we modify the system matrix, as:

$$[A]^T[A]\{U\} = -[A]^T[G]\{\hat{u}^o\} + [A]^T[Q]\{\hat{\varepsilon}\} \tag{34}$$

3.3 Solution procedures

The same iterative procedures which are used in Okada, Fukui & Kumazawa (2001a, 2002) are used in present study. The outlines are briefly presented here. Initial strain iterative procedure, using Eqs. 29 and 33, is adopted to obtain the equilibrium of the unit cell. The initial strain iteration method has often been adopted to analyze elastoplastic problems (see Okada, Rajiyah & Atluri (1988); Okada & Atluri, 1994; Chandra & Mukherjee (1983, 1986)). The procedures of initial strain iteration are summarized as follows.

1. All the displacement gradients or strains of second phase particles in Eq. 33, are set to be zero, as the initial value [all the elements of $\{\hat{\varepsilon}\}$ in Eq. 29 are set to be zero].
2. Eq. 33 is solved for $\{U\}$, and $\left\{u^1\right\}$ and $\{t\}$ are obtained.
3. Strains are evaluated by using Eq. 29, or by the integral Eq. 27.
4. If the norm of change of the strains quantities were small enough,

$$\left|\{\hat{\varepsilon}\}^{\text{Current}} - \{\hat{\varepsilon}\}^{\text{Previous}}\right| \Big/ \left|\{\hat{\varepsilon}\}^{\text{Previous}}\right| < Tol. \tag{35}$$

the iteration is judged to converge. $\{\hat{\varepsilon}\}^{\text{Current}}$ stands for the strains after updated in current iteration step and $\{\hat{\varepsilon}\}^{\text{Previous}}$ are those before updated. $Tol.$ is a small positive number set by the analyst. In present research $Tol.$ is set to be 0.0001. Otherwise, the analysis is repeated from the step 2 above.

It should be noted here that when the elastic moduli (i.e., Young's modulus) of the second phase particles is larger than that of matrix, the above procedures suffer from a convergence problem. That is because the strains (displacement gradients) in the second phase particles become much smaller than those in matrix material. We have overcome this problem by slightly modifying the initial strain iteration algorithm. When the elastic constants for the second phase particles are larger than those for matrix, the strains are updated by:

$$\begin{aligned}&\{\hat{\varepsilon}\}^{\text{Current}}\\&= \frac{1}{(\text{FACT})}\left[\{\hat{\varepsilon}\}-\{\hat{\varepsilon}\}^{\text{Previous}}\right]+\{\hat{\varepsilon}\}^{\text{Previous}}\\&(\text{FACT}) = \frac{Max\left(E^{*I}\right)}{E^{M}}\end{aligned} \tag{36}$$

where $\{\hat{\varepsilon}\}$ represents the strains evaluated in the current iteration step by using Eq. 29 or 27. $E^{*I}\,(I=1,2,3,\cdots,N)$ and E^{M} are the Young's moduli for the second phase particles and matrix materials.

3.4 Effective (homogenized) stresses and elastic moduli

Effective elastic moduli are expressed in Eq. 14 in a general form. When the single-region BEM with volume cells is used for the homogenization analysis, the effective stresses σ^{o}_{ij} due to the macroscopic deformation mode $\partial u^{o}_{k}/\partial x_{\ell}$ are expressed by (see Okada, Fukui & Kumazawa (2001a, 2002)):

$$\begin{aligned}\sigma^{o}_{ij} = \Bigg[&E^{M}_{ijk\ell}+\frac{1}{|Y|}\sum_{I=1}^{N}\int_{\mathrm{Y}^{*_I}}\left(E^{*_I}_{ijk\ell}-E^{M}_{ijk\ell}\right)\mathrm{d}Y^{*_I}\\&+\frac{1}{|Y|}\sum_{I=1}^{N}\int_{\mathrm{Y}^{*_I}}\left(E^{*_I}_{ijmn}-E^{M}_{ijmn}\right)\frac{\partial F_{mk\ell}}{\partial y_n}\mathrm{d}Y^{*_I}\Bigg]\frac{\partial u^{o}_{k}}{\partial x_{\ell}}\end{aligned} \tag{37}$$

Eq. 36 was derived from Eq. 14 by applying Gauss divergence theorem appropriately. The effective elastic moduli are expressed to be:

$$\begin{aligned}E^{H}_{ijk\ell} = &E^{M}_{ijk\ell}+\frac{1}{|Y|}\sum_{I=1}^{N}\int_{\mathrm{Y}^{*_I}}\left(E^{*_I}_{ijk\ell}-E^{M}_{ijk\ell}\right)\mathrm{d}Y^{*_I}\\&+\frac{1}{2\,|Y|}\sum_{I=1}^{N}\int_{\mathrm{Y}^{*_I}}\left(E^{*_I}_{ijmn}-E^{M}_{ijmn}\right)\left(\frac{\partial F_{mk\ell}}{\partial y_n}+\frac{\partial F_{m\ell k}}{\partial y_n}\right)\mathrm{d}Y^{*_I}\end{aligned} \tag{38}$$

It is noted that $F_{ik\ell}$ are determined as the values of u^{1}_{i} by letting each component of $\frac{\partial u^{o}_{i}}{\partial x_{j}}$ be one and all the others be zero (e.g., $\frac{\partial u^{o}_{1}}{\partial x_{1}}=1$ and $\frac{\partial u^{o}_{2}}{\partial x_{1}}=\frac{\partial u^{o}_{3}}{\partial x_{1}}=\frac{\partial u^{o}_{2}}{\partial x_{1}}=\frac{\partial u^{o}_{2}}{\partial x_{2}}=\frac{\partial u^{o}_{2}}{\partial x_{3}}=\frac{\partial u^{o}_{3}}{\partial x_{1}}=\frac{\partial u^{o}_{3}}{\partial x_{2}}=\frac{\partial u^{o}_{3}}{\partial x_{3}}=0$, etc.) in the unit cell analysis.
In present BEM approach, the effective stresses σ^{o}_{ij} can be evaluated in a similar manner.

$$\sigma^{o}_{ij} = \frac{1}{|Y|}\left[E^{M}_{ijk\ell}+\sum_{I=1}^{N}V^{I}\left(E^{*I}_{ijmn}-E^{M}_{ijmn}\right)R^{*I}_{mnk\ell}\right]\frac{\partial u^{o}_{k}}{\partial x_{\ell}} \tag{39}$$

Effective elastic moduli are expressed, as:

$$\begin{aligned}&E^{H}_{ijk\ell}\\&= \frac{1}{|Y|}\left[E^{M}_{ijk\ell}+\frac{1}{2}\sum_{I=1}^{N}V^{*I}\left(E^{*I}_{ijmn}-E^{M}_{ijmn}\right)\left(R^{*I}_{mnk\ell}+R^{*I}_{mn\ell k}\right)\right]\end{aligned} \tag{40}$$

where $R^{*I}_{ijk\ell}$ are the characteristic functions expressing the strains in the I-th particle, as:

$$\hat{\varepsilon}^{I}_{ij} = R^{*I}_{ijk\ell}\frac{\partial u^{o}_{k}}{\partial x_{\ell}} \tag{41}$$

$R^{*I}_{ijk\ell}$are computed in the same way as $F_{ijk\ell}$ are evaluated.

4 Numerical results

4.1 One particle problem

First, a simple problem is solved to compare the results of present BEM formulation with those of multi-region BEM (Okada, Fukui & Kumazawa (2001a, 2002)) calculations. A spherical particle located at the center of the unit cell is assumed, as shown in **Figure 8**. The size and elastic modulus of the particle are varied and the accuracy of present formulation is discussed. Matrix and the particle are isotropic and the Poisson's ratios for both the materials are assumed to be 0.3. 36 (6 by 6) linear quadrilateral boundary elements are placed on each face of the cube. There are a total of 216 boundary elements on the outer faces of the unit cell.

Analysis models for present BEM and for the multi-domain BEM analyses are shown in **Figures 9** and **10**. It is noted that when present formulation is used only

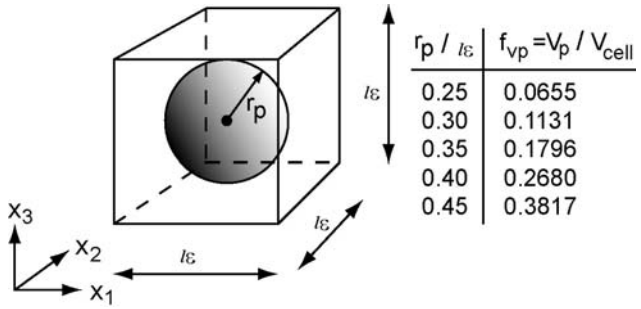

r_p / ℓ_ε	$f_{vp}=V_p / V_{cell}$
0.25	0.0655
0.30	0.1131
0.35	0.1796
0.40	0.2680
0.45	0.3817

Figure 8 : One particle problem to compare the results of present method and those of multi-region BEM

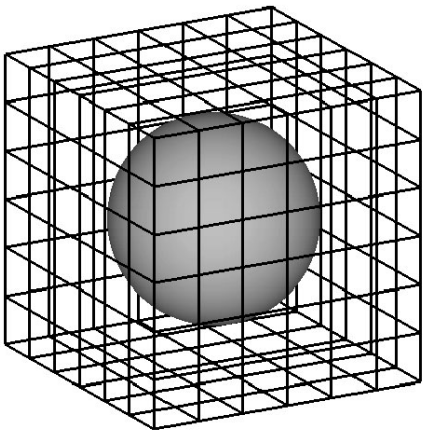

Figure 9 : Boundary discretization and a particle for the one particle model which is solved by present BEM approach

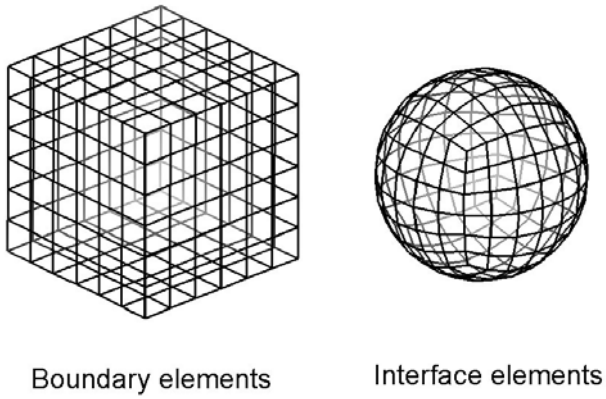

Figure 10 : Boundary and interface discretizations for the one particle problem which is solved by multi-region BEM approach

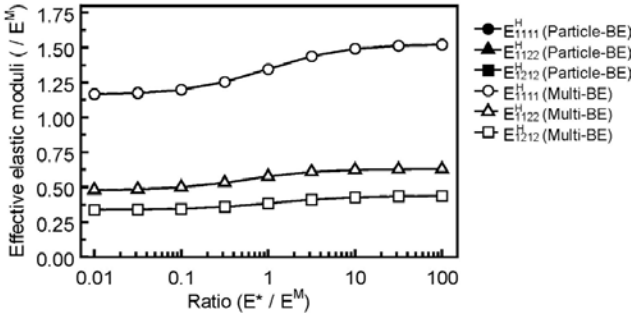

Figure 11 : The variations of effective elastic constants (E^H_{1111},E^H_{1122} and E^H_{1212}) with respect to that of the ratio E^*/E^M of Young's moduli for the case $r_p/\ell_\varepsilon = 0.25$

the location and the size of spherical particle are specified and there is no volume discretization. The particle is shown by an illustration. For the multi-region BEM analysis, we need to discretize the interface between the particle and matrix by boundary elements. We have 216 linear quadrilateral interface elements. The ratio of the radius r_p of particle and the size ℓ_ε of unit cell are set to be 0.25, 0.30, 0.35, 0.40 and 0.45 and their corresponding volume fraction of the particle are 6.55%, 11.31%, 17.96%, 26.80% and 38.17%. The ratio E^*/E^M of the Young's moduli of the particles and matrix are varied from 0.01 to 100. The case of $E^*/E^M = 0.01$ represents a case where the particle is so soft that this case almost represents the problem of a spherical void. In the case of $E^*/E^M = 100$, the particle is so stiff that this case almost represents the case of spherical rigid particle.

We first present the variations of effective elastic constants (E^H_{1111},E^H_{1122} and E^H_{1212}) with respect to the change of the ratio E^*/E^M are presented for r_p/ℓ_ε being 0.25, 0.35 and 0.45. In **Figures 11**, **12** and **13**. The results obtained by present method and by the multi-region BEM formulation are indicated by "Particle-BE" and "Multi-BE", respectively. It is seen that the value of r_p/ℓ_ε is equal or less than 0.35 (volume fraction is equal to or less than 17.96%), the results of present and multi-region BEM formulations are in a perfect match. However, for the case of r_p/ℓ_ε being 0.45 (volume fraction is 38.17%), the results of present formulation differ from those of multi-region BEM. The discrepancies may be caused by the assumption of uniformly distributed stresses and strains within a particle. The distance between the boundary of the unit cell and the particle becomes so small that the assumption breaks down. Then, some comparisons are made on the variations of effec-

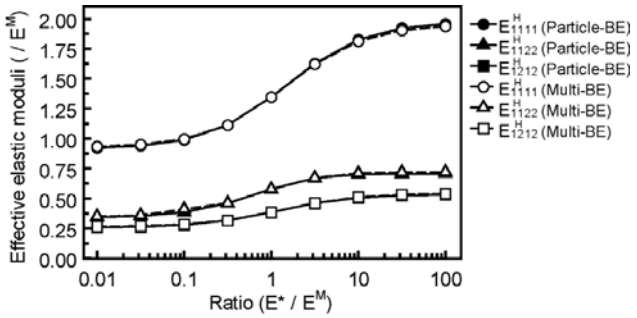

Figure 12 : Variations of effective elastic constants $(E^H_{1111}, E^H_{1122}$ and $E^H_{1212})$ with respect to that of the ratio E^*/E^M of Young's moduli for the case $r_p/\ell_\varepsilon = 0.35$

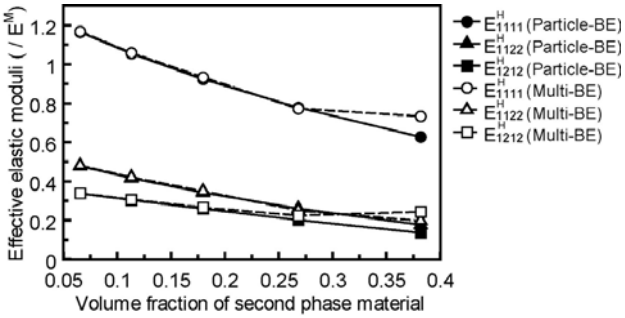

Figure 14 : Variations of effective elastic constants $(E^H_{1111}, E^H_{1122}$ and $E^H_{1212})$ with respect to the ratio r_p/ℓ_ε of the radius of particle and the size of unit cell for $E^*/E^M = 0.01$

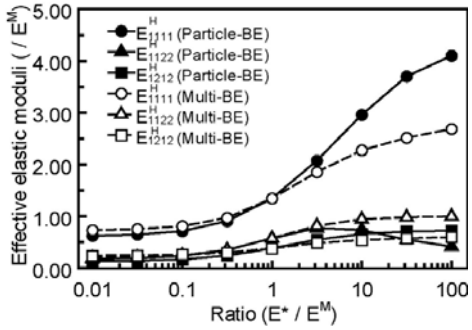

Figure 13 : Variations of effective elastic constants $(E^H_{1111}, E^H_{1122}$ and $E^H_{1212})$ with respect to that of the ratio E^*/E^M of Young's moduli for the case $r_p/\ell_\varepsilon = 0.45$

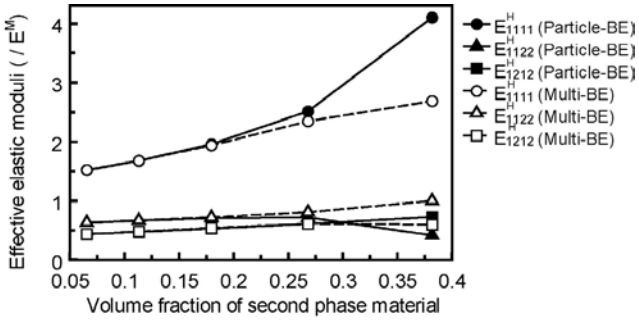

Figure 15 : Variations of effective elastic constants $(E^H_{1111}, E^H_{1122}$ and $E^H_{1212})$ with respect to the ratio r_p/ℓ_ε of the radius of particle and the size of unit cell for $E^*/E^M = 100$

tive moduli with respect to the that of the volume fraction of the particle. In **Figures 14** and **15**, the variations are plotted for the cases of E^*/E^M being equal 0.01 and 100. The results of both the methods (present and multi-region BEM) are almost identical to each other when the volume fraction is equal or less than 0.268. However, especially for $E^*/E^M = 100$, large discrepancies between the results are seen. Therefore, it can be said that present method can serve reasonably accurate solutions when the volume fraction of the particles is smaller than 26%.

The distributions of stress are presented for the case $r_p/\ell_\varepsilon = 0.35$ with $E^*/E^M = 0.01$ and $E^*/E^M = 100$. A two dimensional finite element-like mesh is generated in the cross section of the unit cell. The plane of visualization includes the center of the spherical particle and it is perpendicular to the x_3 axis. The distributions of σ_{11} under macroscopic deformation mode $\partial u^o_1/x_1 = 1$ are visualized. It is noted here that the case with $E^*/E^M = 0.01$ (shown in **Figure 16 (a)**) almost corresponds to the case of spherical void. $E^*/E^M = 100$ (**Figure 16 (b)**) indicates that there is an almost rigid inclusion. For $E^*/E^M = 0.01$, it is seen from **Figure 16 (a)** that stress σ_{11} is almost zero inside the particle and at both the sides of particle the stress in matrix is almost zero (the value is slightly negative, but its magnitude is very small). There is no unacceptable jump in stress value at the interface. Also, we find stress concentration in matrix at the top and bottom of the particle. From **Figure 16 (b)**, the stress σ_{11} inside of the particle is significantly larger than average stress in matrix. At the top and bottom of the particle, the stress is almost zero. For both the cases, we do not find any unacceptable stress jump at the interface and the distributions of stress are as expected.

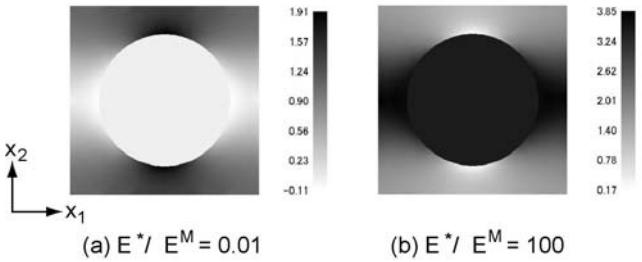

Figure 16 : Distributions of stress σ_{11} normalized by E^M for macroscopic deformation mode $\partial u_1^o/\partial x_1 = 1$ in the cross section of the unit cell. (a) $E^*/E^M = 0.01$ and (b) $E^*/E^M = 100$

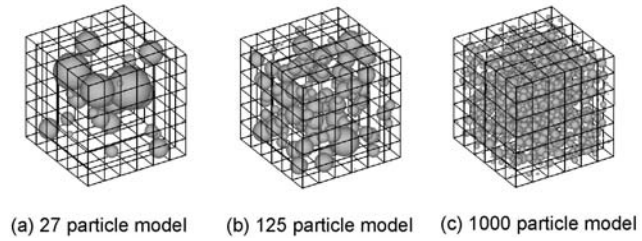

Figure 17 : (a) 27, (b) 125 and (c) 1000 particle model

4.2 Randomly distributed particles

The problems of randomly distributed spherical particles are considered in this section. Three models are analyzed as shown in **Figure 17 (a)**, **(b)** and **(c)**. The volume fractions of the particles are 12% for 27 particle model, 15% for 125 particle model and 15% for 1000 particle model. To distribute the particles, we adopted Sobol' sequence (Press, Teukolsky, Vetterling & Flannery (1996)), which is a method to evenly distribute points in a multi dimensional space. The sizes of the particles are determined such that the radius of a particle is set to be a fraction of distance to the center of the nearest particle. The fraction is adjusted so that the volume fraction becomes the specified value. For the case of 27 particle problem, the highest possible volume fraction we could set was about 13%. When the value of volume fraction which is larger than 13% is specified, some particles overlap each other.

For a class of problems in which the particles randomly distribute in the unit cell, it is extremely difficult to obtain solutions by using the finite element method or by the boundary element method. And there is no exact solution to compare with. We take the solutions of self-consistent method and Eshelby's method (see, Mura (1982)) as our references.

The results are presented in **Figures 18 (a)**, **(b)** and **(c)**. The effective Young's modulus are plotted for the variation of the ratio E^*/E^M of Young's moduli of particles and matrix. The trends of the results which are obtained by present BEM approach are very similar to those of the reference solutions. Therefore, the solutions of present BEM approach are proven to be reliable.

Stress distributions in the cross section of the unit cell (125 particle model) are presented in **Figure 19**. Two dimensional finite element-like mesh is generated in the cross section and then the distributions of stress are drawn. In **Figure 19 (a)**, the distributions of stress σ_{11} for $E^*/E^M = 0.01$ and $\partial u_1^o/\partial x_1 = 1$ (and all the others are zero) in $y_2 = 5$ plane, is shown. In **Figure 20 (b)**, the distribution of σ_{11} is plotted for $E^*/E^M = 100$. It is seen that the stress distributions in matrix is very complex, and, especially for the case of $E^*/E^M = 0.01$, stress concentrations at the sides of the particles (voids) are found. In **Figure 19 (b)**, the particles are found to have a large magnitude of stress.

5 Conclusions

A new BEM formulation for the analysis of particulate composite materials is presented in this paper. Present formulation can analyze the problems of unit cell which contain a number of distributed particles. The number of distributed particles, which are demonstrated in this paper, is up to 1000. By using BEM in a traditional way (i.e., multi-region BEM) for the analyses of heterogeneous materials, such a huge RVE would extremely be difficult to deal with. In present approach, there are a certain level of simplification such as the uniformly distributed stresses and strains in each particle, is introduced. The effective properties obtained by present approach are accurate when the volume fraction of the particles is less than about 25%.

The results presented in this paper are rather simple cases. For example, with present formulation, one may analyze the problems of stress induced phase transformation (see Okada, Fukui & Kumazawa (2001b)). Macroscopic stress-strain curve may be obtained based on the evolution of microstructure. In the authors' forthcoming paper, we apply present BEM approach to such nonlinear problems.

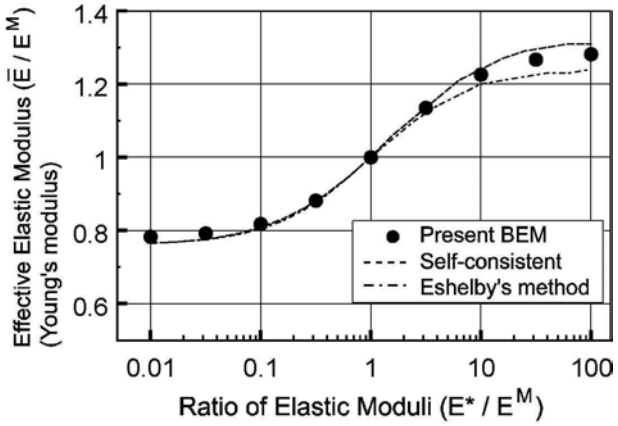

(a) 27 particle model

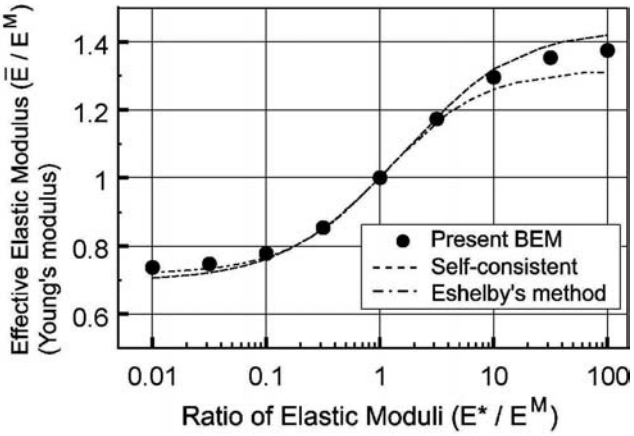

(b) 125 particle model

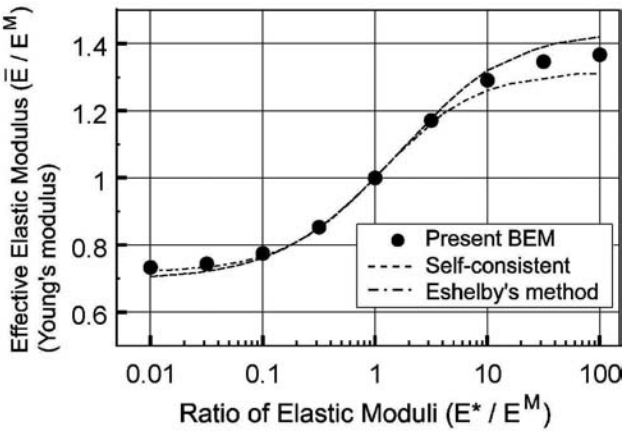

(c) 1000 particle model

Figure 18 : The variations of effective Young's modulus calculated by (a) 27, (b) 125 and (c) 1000 particle model with respect to the variation of the ratio E^*/E^M

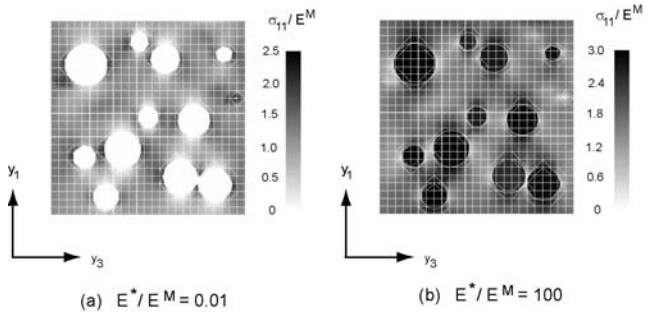

Figure 19 : The distribution of stress σ_{11} for $E^*/E^M = 0.01$ and $\partial u_1^o/\partial x_1$ (and all the others are zero) in $y_2 = 5$ plane

6 References:

Ashby, M. F.(1993): Criteria for selecting the components of composites, *Acta Metall. Mater,* vol. 41, pp. 1313-1335.

Atluri, S. N.; Han, Z. D.; Shen, S. (2003): Meshless Local Patrov-Galerkin (MLPG) approaches for weakly-singular traction & displacement boundary integral equations, *CMES: Computer Modeling in Engineering & Sciences*, vol. 4, no. 5, pp. 507-517.

Banerjee, P.K.; Butterfield, R. B. (1981): *Boundary Element Methods in Engineering and Science*, McGraw-Hill, UK.

Banerjee, P.K.; Cathie, D.N. (1980): A direct formulation and numerical implementation of the boundary element method for two-dimensional problems of elasto-plasticity, *Int. J. Mech. Sci* , vol. 22, pp. 233-245.

Banerjee, P.K.; Henry, D.P. (1992): Elastic analysis of three-dimensional solids with fiber inclusions by BEM, *Int. J. of Solids Struct.*, vol. 29, pp. 2423-2440.

Banerjee, P.K.; Reveendra, S.T. (1987): New boundary element formulation for 2-D elastoplastic analysis, *Journal of Engineering Mechanics*, vol. 113, no. 2, pp. 252-265.

Bensoussan, A.; Lions, J.-L.; Papanicolaou, G. (1978): *Aymptotic analysis for periodic structures, Studies in mathematics and its applications vol. 5*, North-Holland, Amsterdam.

Chandra, A.; Mukherjee, S. (1983): Applications of the boundary element method to large strain large deformation problems of viscoplasticity, *Journal of Strain Analysis*, vol. 18, no. 4, pp. 261-270.

Chandra, A.; Mukherjee, S. (1986): An analysis of large strain viscoplasticity problems including the effects of induced material anisotropy, *Journal of Applied Mechanics*, vol. 53 pp. 77-82

Chung, P. W.; Namburu, R. R.; Henz, B. J. (2004): A Lattice Statics-Based Finite Element Method, *CMES: Computer Modeling in Engineering & Sciences*, Vol. 5, No. 1, pp. 45-62.

Cruse, T.A. (1969): Numerical solutions in three dimensional elastostatics, *Int. J. of Solids Struct*, vol. 5, pp. 1259-1274.

Eshelby, J.D. (1957): The determination of the elastic field of an ellipsoidal inclusion, and related problems, Proceedings of Royal Society, London, vol. A24, pp. 376-396.

Fish, J. (1992): The *S*-Version of the Finite Element Method, *Computers & Structures*, vol. 43, pp. 539-547.

Fish, J., Guttal, R. (1996): The $_S$-Version of Finite Element Method for Laminated Composites, *International Journal for Numerical Methods in Engineering*, vol. 39, pp. 3641-3662.

Guedes, J. M.; Kikuchi, N. (1990): Preprocessing and postprocessing for Materials based on the homogenization method with adaptive finite element methods, *Comput. Method Appl. Mech. Eng.*, Vol. 83, pp. 143-198.

Han, D. Z.; Atluri, S. N. (2003): On simple formulation of weakly singular traction & displacement BIE, and their solutions through Petrov-Galerkin Approaches, *CMES: Computer Modeling in Engineering & Sciences*, vol. 4, no. 1, pp. 5-20.

Higa, Y.; Tomita, Y. (2000): Modeling and Computational Simulation of Deformation Behavior of Particulate-Reinforced Composite Materials by Homogenization Method (in Japanese), *Trans. JSME Series A*, vol. 66, no. 648, pp. 1441-1446.

Hollister, S.J.; Kikuchi, N. (1992): A Comparison of homogenizetion and standard mechanics analyses for periodic porous composites, *Comput. Mech.*, vol. 10, pp. 73-95.

Hollister, S.J.; Kikuchi, N. (1994): Homogenization theory and digital imaging: a basis for studying the mechanics and design principles of bone tissue, *Biotechnology and Biongineering*, vol. 43, pp. 586-596.

Kalamkarov, A. L. (1992): *Composite and Reinforced Elements of Construction*, John Wiley & Sons, Chichester, England.

Kamiski, M. (1999): Boundary Element method homogenization of the periodic linear elastic fiber composites, *Engineering Analysis with Boundary Elements*, vol. 23, pp. 815-823.

Kane, J. H. (1994): *Boundary Element Analysis in Engineering Continuum Mechanics*, Prentice Hall, Englewood Cliffs, NJ.

Kato, T.; Nishioka, T. (2000): Analysis of Damaged Materials Containing Numerous Elliptical Cracks by Using the Homogenization Method (in Japanese), *Trans. JSME Series A*, vol. 66, no. 643, pp. 524-531.

Lee, K.; Moorthy, S.; Ghosh, S. (1999): Multiple scale computational model for damage in composite materials, *Comput. Method Appl. Mech. Eng*, vol. 172, pp. 175-201.

Moorthy, S.; Ghosh, S. (1998): A Voronoi cell finite element model for particle craking in elastic-plastic composite materials, *Comput. Method Appl. Mech. Eng.*, vol. 151, pp. 377-400.

Mura, T. (1982): *Mechanics of Defects in Solids*, Martinus Nijhoff Publications, London.

Nishioka, T.; Kato, T. (1998): An alternating method based on the VNA solution for analysis of damaged solid containing arbitrarily distributed elliptical microcracks, *International Journal of Fracture*, vol. 89, pp. 159-192.

Ohno, N.; Matsuda, T.; Wu, X. (2001): A homogenization theory for elastic-viscoplastic composites with point symmetry of internal distributions, *Int. J. of Solids Struct.*, vol. 38, pp. 2867-2878.

Ohno, N.; Wu, X.; Matsuda, T. (2000): Homogenized properties of elastic-viscoplastic composites with periodic internal structures, *International Journal of Mechanical Sciences*, vol. 42, pp. 1519-1536.

Ohno, N.; Okumura, D.; Noguchi, H. (2002): Microscopic Symmetric bifurcation condition of cellular soids based on a homogenization theory of finite defromation, *Journal of the Mechanics and Physics of Solids*, vol. 50, pp. 1125-1153.

Okada, H.; Atluri, S.N. (1994): Recent developments in the field-boundary element method for finite/small strain elastoplasticity, *International Journal of Solids and Structures*, vol. 31, pp. 1737-1775.

Okada, H.; Fujitani, S.; Fukui, Y.; Kumazawa, N. (2001): Analysis of Beam/Bar Structure based on Ho-

mogenization method (in Japanese), *Trans JSME Series A*, vol. 67, no. 658, pp. 933-939.

Okada, H.; Fukui, Y.; Kumazawa, N.; Maruyama, T. (1998): Homogenization Method for Nonlinear Materials undergoing Large Deformation (1st Report, Mathematical Formulations, Which can Rigorously Satisfy the Assumption of Periodicity) (in Japanese), *Trans JSME Series A*, vol. 64, no. 618, pp. 450-456.

Okada, H.; Fukui, Y.; Kumaszawa, N. (2000): Formulations for Homogenization Method Based on Boundary Element Method, Advances in Computational Engineering and Sciences Edt. by Brust and Atluri, pp. 1128-1133.

Okada, H.; Fukui, Y.; Kumazawa, N. (2001a): Homogenization method for heterogeneous material based on boundary element method, *Comput. Struct.*, vol. 79, pp. 1987-2007.

Okada, H.; Fukui, Y.; Kumazawa, N. (2001b): A boundary element based meso-analysis on the evolution of material damage, in Advances in Fracture Research (Proceedings of ICF10 International Conference on Fracture) eds. K. Ravi-Chandar, B.L. Karihaloo, T. Kishi, R.O. Ritchie, A.T. Yokobori Jr., T. Yokobori, Pergamon (an imprint of Elsevier Science), CD-ROM.

Okada, H.; Fukui, Y.; Kumazawa, N. (2002): Homogenization Analysis using the Boundary Element Method (Formulations and Computer Implementation in Elastic Analysis) (in Japanese), *Trans JSMA Series A*, vol. 68, no. 666, pp. 181-188.

Okada, H.; Rajiyah, H.; Atluri, S.N. (1990): A full tangent stiffness field-boundary element formulation for geometric and material nonlinear problems of solid mechanics, *International Journal for Numerical Methods in Engineering*, vol. 29, pp. 15-35.

Okada, H.; Rajiyah, H.; Atluri, S.N. (1988): Some recent development in finite-strain elastoplasticity using the field-boundary element method, *Computers & Structures* vol. 30 (1/2), pp. 275-288.

Press, W.H.; Teukolsky, S. A.; Vetterling, W. T.; Flannery, B. P. (1996): *Numerical Recipes in Fortran 77*, Cambridge University Press, Cambridge, UK.

Procházka, P. (2001): Homogenization of linear and of debonding composites using BEM, *Engineering Analysis with Boundary Elements*, vol. 25, pp. 753-769.

Raghavan, P.; Ghosh, S. (2004): Adaptive Multi-scale Computational Modeling of Composite Materials, *CMES: Computer Modeling in Engineering & Sciences*, Vol. 5, No. 2, pp. 151-170.

Rizzo, F.J. (1967): An integral equation approach to boundary value problems of classical elastostatics, *Quarterly of Applied Mathematics*, vol. 25, pp. 83-95.

Shibuya, Y.; Wang, S.-S. (1994): Nonlinear Behavior of Metal Matrix Fiber Composites with Damage on Interface (in Japanese), *Trans. JSME Series A*, vol. 60, no. 569, pp. 153-158.

Silva, E.C.N.; Nishiwaki, S., Fonseca, J. S. O., Kikuchi, K. (1999): Optimization methods applied to material and Flextensional actuator design using the homogenization method, *Comput. Method Appl. Mech. Eng*, vol. 172, pp. 241-271.

Takano, N.; Ohnishi, Y.; Zako, M.; Nishiyabu, K. (2000): The formulation of homogenization method applied to large deformation problem for composite materials, *Int. J. of Solids Struct.*, vol. 37, pp. 6517-6535.

Takano, N.; Ohnishi, Y.; Zako, M.; Nishiyabu, K. (2001): Microstructure-based deep-drawing simulation of knitted fabric reinforced thermoplastics by homogenization method, *Int. J. of Solids Struct.*, vol. 38, pp. 6333-6352.

Takano, N.; Zako, M.; Kikuchi, N. (1995): Stress analysis of sandwich plate by the homogenization method, *Materials Science Research International*, vol. 1, no. 2, pp. 82-88.

Terada, K.; Hori, M.; Kyoya, T.; Kikuchi, N. (2000): Simulation of the multi-scale convergence in computational homogenization approaches, *Int. J. of Solids Struct.*, vol. 37, pp. 2285-2311.

Terada, K.; Miura, T.; Kikuchi, N. (1997): Digital image-based modeling applied to the homogenization analysis of composite materials, *Computational Mechanics*, vol. 20, pp. 331-346.

Wienecke, H.A.; Brockenbrough, J.R.; Romanko, A.D. (1995): A Three-dimensional unit cell model with application toward particulate composites, *Journal of Applied Mechanics*, vol. 63, pp. 136-140.

Wu, X.; Ohno, N. (1999): A Homogenization Theory for time-dependent nonlinear composites with periodic internal structures, *Int. J. of Solids Struct.*,vol. 36, pp. 4991-5012.